

This document is made available through the declassification efforts
and research of John Greenewald, Jr., creator of:

The Black Vault



The Black Vault is the largest online Freedom of Information Act (FOIA) document clearinghouse in the world. The research efforts here are responsible for the declassification of hundreds of thousands of pages released by the U.S. Government & Military.

Discover the Truth at: <http://www.theblackvault.com>

LA-UR- 04-1191

Approved for public release;
distribution is unlimited.

Title: OPTIMIZATION OF CHEMICAL ETCHING PROCESS IN
NIOBIUM CAVITIES

Author(s): TSUYOSHI TAJIMA, LANSCE-1
MOHAMED B. TRABIA, UNLV
WILLIAM CULBRETH, UNLV
SATHISH K. SUBRAMANIAN, UNLV

Submitted to: INTERNATIONAL DESIGN ENGINEERING TECHNICAL
CONFERENCE, SALT LAKE CITY, UTAH,
SEPTEMBER 28-OCTOBER 2, 2004



Los Alamos National Laboratory, an affirmative action/equal opportunity employer, is operated by the University of California for the U.S. Department of Energy under contract W-7405-ENG-36. By acceptance of this article, the publisher recognizes that the U.S. Government retains a nonexclusive, royalty-free license to publish or reproduce the published form of this contribution, or to allow others to do so, for U.S. Government purposes. Los Alamos National Laboratory requests that the publisher identify this article as work performed under the auspices of the U.S. Department of Energy. Los Alamos National Laboratory strongly supports academic freedom and a researcher's right to publish; as an institution, however, the Laboratory does not endorse the viewpoint of a publication or guarantee its technical correctness.



OPTIMIZATION OF CHEMICAL ETCHING PROCESS IN NIOBIUM CAVITIES

M. Trabia, W. Culbreth, S. Subramanian, T. Tajima*
Department of Mechanical Engineering
Howard R. Hughes College of Engineering
University of Nevada, Las Vegas
Las Vegas, NV 89154-4027

Tel: (702) 895-0957, Fax: (702) 895-3936, Email: mbt@me.unlv.edu

*Los Alamos National Laboratory, Los Alamos, NM 87545

Abstract-Superconducting niobium cavities are important components of linear accelerators. Buffered chemical polishing (BCP) on the inner surface of the cavity is a standard procedure to improve its performance. The quality of BCP, however, has not been optimized well in terms of the uniformity of surface smoothness. A finite element computational fluid dynamics (CFD) model was developed to simulate the chemical etching process inside the cavity. The analysis confirmed the observation of other researchers that the iris section of the cavity received more etching than the equator regions due to higher flow rate. The baffle, which directs flow towards the walls of the cavity, was redesigned using optimization techniques. The redesigned baffle significantly improves the performance of the etching process. To verify these results an experimental setup for flow visualization was created. The setup consists of a high speed, high resolution CCD camera. The camera is positioned by a computer-controlled traversing mechanism. A dye injecting arrangement is used for tracking the fluid path. Experimental results are in general agreement with CFD and optimization results.

I. INTRODUCTION

The nuclear industry provides a significant percentage of the world, as well as of the United States, with electricity. Nuclear power plants produce thousands of tons of spent fuel. Some of this spent fuel can be radioactive for thousands of years. The US DOE is currently exploring the possibility of creating a permanent storage site at Yucca Mountain, Nevada, for spent nuclear fuel. The US Congress has recently authorized exploring an alternative way to deal with spent nuclear fuel: Accelerator Transmutation of Waste (ATW). In this approach, a particle accelerator produces protons that react with a heavy metal target to produce neutrons that hit spent fuel and shorten the life of radioactivity through nuclear reactions. A major component of the system is a linear accelerator (linac) that can accelerate over 100 mA of protons to several GeV [1]. Los

Alamos National Laboratory (LANL) is an active participant in developing a high-current superconducting rf (SCRF) linear accelerator. It has three major components: niobium cavities, power couplers, and cryo modules. This paper principally deals with niobium cavities.

Niobium cavities have several advantages including significantly small power dissipation compared to copper cavities due to the superconductivity. These cavities are usually made of multiple elliptical cells, Figure 1. They are formed from sheet metal using various techniques such as deep drawing or spinning. The cells then are welded together using electron-beams. Multi-cell units are usually tuned by stretching or squeezing them.

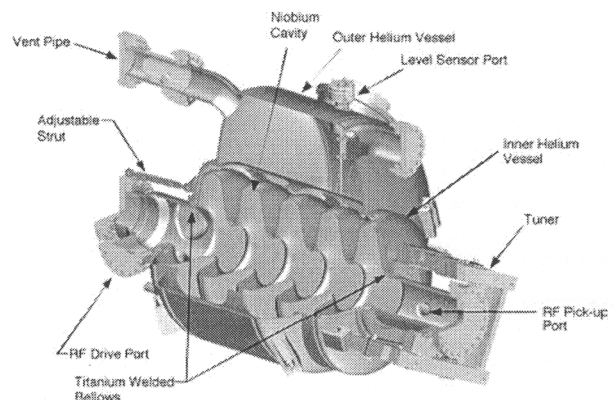


Figure 1. A LANL APT Five-Cell Niobium Cavity Assembled with Helium Vessels.

The performance of a niobium cavity deteriorates if its surface has stains of chemical products on the surface. Insufficient degreasing, liquid retention in pits, areas with varying metal structure introduced during the manufacturing, or

mechanical surface damage also affect the performance. Foreign particles sticking to the cavity surface also cause field emission that degrades the cavity performance. To ensure the success of the niobium cavities, they are chemically polished and then subjected to high pressure rinsing, [2]. Palmieri, [3], stated that chemical etching is the industry standard. The following is a brief overview of some of the research activities in this area. Kneisel [4] compared chemical etching to electro polishing. He presented etching rates for different etching fluids. Ono [5] studied the effects of many factors including chemical polishing on the performance of superconducting cavities. He concluded that chemical etching might not improve the performance after a certain depth ($\cong 100 \mu\text{m}$). Kneisel and Palmieri, [6], however, stated that good performance of seamless cavities requires removal of a relatively large amount of material removal. Singer et al. [7] used a combination of electro polishing and chemical etching to improve the surface quality. Aune et al. [8] presented a comprehensive study on developing nine-cell cavity. They applied chemical etching to the surface of the cavity during different stages of manufacturing. The researchers noticed that the surface of the cavity experiences more etching near the iris than near the equator of the cavity. To improve the uniformity of the etching process, researchers at Los Alamos National Laboratory (LANL) proposed inserting a baffle inside the cavity to help direct the etching fluid toward the equator walls of the cavity, Figure 2. The objectives of this paper are,

- (i) Evaluate the effectiveness of LANL design using a computational fluid dynamics (CFD).
- (ii) Propose an alternative baffle design if needed
- (iii) Optimize the baffle design to improve the uniformity of the flow speed on the cavity surface.
- (iv) Visualize and verify the CFD results using an experimental setup composed of a transparent prototype of the cavity, fabricated optimized baffle, CCD camera and a traversing mechanism for positioning the camera.

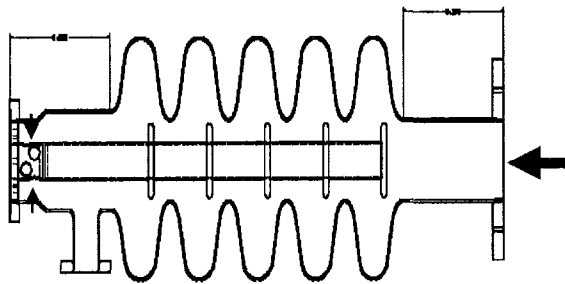


Figure 2. Current Etching Configuration of Niobium Cavities.

II. BACKGROUND

The composition of the etching fluid is presented in Table I. The etching fluid has the following characteristics:

Density= 1532 kg/m^3

Dynamic Viscosity= 0.0221 Ns/m^2

Average inlet velocity is 0.0475 m/s . The etching fluid is actively chilled in a reservoir after it exits the cavity. Temperature is maintained below 15°C . The flow is moving against gravity. The fluid leaves the cavity through holes in the baffle.

Table I. Chemical Composition of the Etching Fluid

Part Volume)	Acid	Reagent Grade
1	Nitric Acid (HNO_3)	(69-71%)
1	Hydrofluoric Acid (HF)	(48%)
2	Phosphoric Acid (H_3PO_4)	(85%)

III. PERFORMANCE INDEX

Internal boundaries are created close to the inner walls of the cavity, Figure 3. Each cell is divided into six sections as can be seen in the zoomed-in view in the same figure:

- Bottom iris
- Bottom straight
- Bottom equator
- Top equator
- Top straight
- Top iris

Inlet and outlet sections are represented using one boundary each. The velocity is integrated along each section. A performance index is defined using two quantities. The first quantity describes the average velocity along the internal boundaries of the cavity surface while the second one defines its standard deviation. The objective of the optimization is to maximize the first and minimize the second variable as follows:

$$PI = F \left(\frac{v_{av}}{\frac{\sum_{i=1}^n \int v ds}{\int ds}} \right) + \sqrt{\frac{\sum_{i=1}^n \left[\frac{\int v ds}{\int ds} - VEL \right]^2}{n}} \quad (1)$$

where, v_{av} is the average inlet velocity.

n is the number of boundaries (total of thirty-two).

F is a factor to allow combining the two quantities in the same performance index.

VEL is the average velocity of all the internal boundaries.

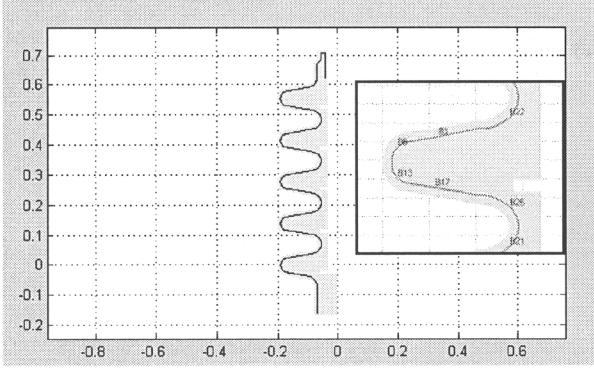


Figure 3. Internal Boundaries of the Cavity (inset: zoomed-in view of a cavity)

A computational fluid dynamics model of the cavity with the baffle was developed. The problem was modeled as a two-dimensional, axisymmetric, steady state fluid flow problem. Figure 4 shows the velocity field for the current baffle design. The results showed that the baffle succeeded in directing the flow toward the cavity surface. The flow was, however restricted to the neighborhood of the iris regions with very limited circulation in the equator regions, which confirms the observations of Aune et al. [8]. The current design also experiences back flow behind the second through fifth cells. There is a significant increase in velocity at the outlet. Average velocity is equal to 0.0482 m/s while the standard deviation is 0.2422.

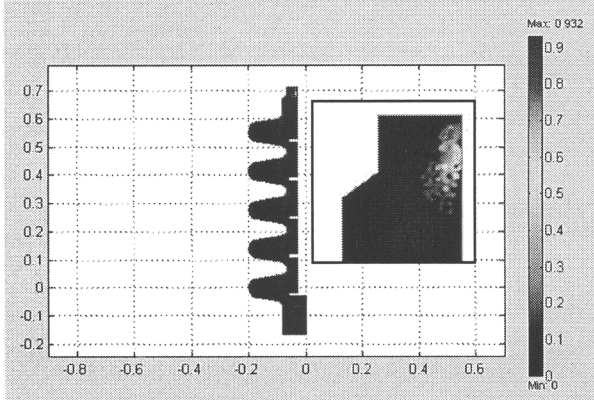


Figure 4. Velocity Field for the Current Baffle Design (inset: zoomed-in view of the flow at the exit)

IV. ALTERNATIVE BAFFLE DESIGN

To design an alternative baffle all possible variables are identified in Figure 5. These variables are listed in Table II. The new design allows baffle to penetrate into the cells to improve etching. Baffle discs can be sloped to better direct the flow. Additionally the flow leaves through the cavity outlet instead of holes in the baffle to reduce the exit velocity.

Table II. Baffle variables

Variable	Description
x_1	Location of the first baffle relative to the equator of first cell
x_2	Thickness of the baffle
x_3	Spacing between baffles
x_4	Radius of the pipe
x_5	Distance from pipe center to the end of the taper
x_6	Extension of the baffle from the taper
x_7	Baffle bottom angle at inlet
x_8	Baffle top angle from first through fourth cell
x_9	Baffle bottom angle from second through fifth cell.
x_{10}	Baffle top angle at fifth cell

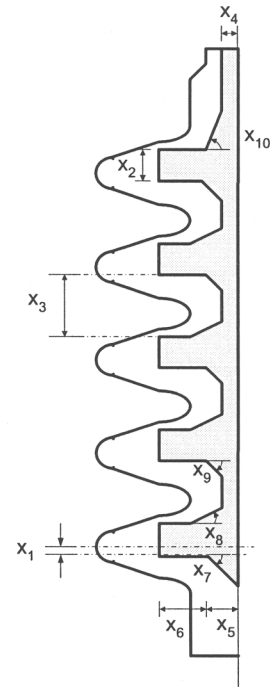


Figure 5. Baffle variables

V. SENSITIVITY OF VARIABLES

Using finite difference, sensitivity of variables is assessed. A variable is more sensitive to the etching process if the rate of change of average velocity or rate of change of standard deviation is high. Results show that except for the angles, all other variables are sensitive. It is therefore decided to optimize x_1 through x_6 .

VI. OPTIMIZATION OF THE BAFFLE VARIABLES

Inequality constraints are used to ensure realistic solution. These constraints are listed below:

$$-0.022 < x_1 < 0 \text{ m} \quad (2)$$

$$0 < x_2 < 0.044 \text{ m} \quad (3)$$

$$0.094 < x_3 < 0.138 \text{ m} \quad (4)$$

$$0.01 < x_4 < 0.04 \text{ m} \quad (5)$$

$$0.01 < x_5 < 0.06 \text{ m} \quad (6)$$

$$0 < x_6 < 0.8 x_5 \quad (7)$$

The upper bound in the sixth set of constraints indicates the physical limits of the length of the extended portion of the baffle.

Additional constraints ensure that the baffle does not intersect the cavity walls of Figure 3. These constraints are created by representing each segment of the internal boundaries of the cavity and the baffle using line parametric form:

$$\begin{cases} x \\ y \end{cases} = \begin{cases} x_s \\ y_s \end{cases} + u \begin{cases} x_f - x_s \\ y_f - y_s \end{cases} \quad 0 \leq u \leq 1 \quad (8)$$

Where, (x_s, y_s) and (x_f, y_f) are the starting and final point of segment respectively. Possibility for intersection between two segments, a and b , is checked by solving their parametric equations simultaneously. If both u_a and u_b are between *zero* and *one*, intersection occurs. Since the quality of the mesh changes for each set of variables, an additional constraint is needed to ensure that the results of the finite-element model are reasonable. This constraint compares the flow rate in inlet and exit of the cavity as follows,

$$|Q_i - Q_e| \leq 0.02 Q_i \quad (9)$$

Where, Q_i and Q_e are the flow rates at inlet and outlet of the cavity respectively. Flow rate at exit is calculated by integrating velocity over exit area. A total of fifteen constraints are included in the objective function using penalty terms. The modified objective function is,

$$\begin{aligned} \text{minimize,} \quad & FC = PI + \sum_{i=1}^m \Omega_i \\ \text{if } g_i(x) \leq 0 \quad & \Omega_i = R * g_i(x)^2 \\ \text{if } g_i(x) > 0 \quad & \Omega_i = 0 \end{aligned} \quad (10)$$

R is the penalty parameter, whose value is 10^{15} . $g_i(x)$ is equation of constraint i . Fuzzy Simplex Algorithm [9] is used to optimize this problem since it usually provides lesser number of function evaluations with comparable problems.

The following data are used as an initial estimate for the modified baffle design:

$$\{x\}^T = \{-0.006, 0.012, 0.126, 0.015, 0.055, 0.04\}^T$$

Average velocity is equal to 0.0324 m/s while the standard deviation is 0.2072. Results, Figure 6, show that backflow is eliminated. The flow is also closer to the surface of the cavity.

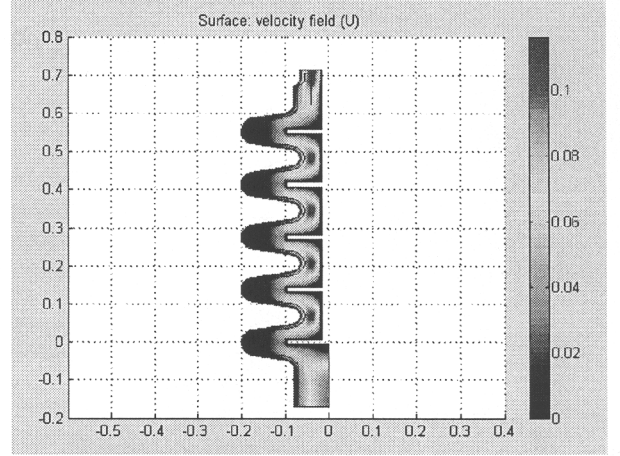


Figure 6. Velocity Field for the Initial Guess of the Modified Baffle Design

The algorithm reached the optimized solution after 738 function evaluations:

$$\{x\}^T = \{-0.022, 0.044, 0.094, 0.0128, 0.060, 0.0480\}^T$$

Average velocity in this case is equal to 0.0553 m/s while the standard deviation is 0.1854. Test points in the neighborhood of this point consistently have higher function value. Results of the optimized design are shown in Figure 7. These results and many other attempts lead to the following observations:

1. The thickness of the baffle, x_2 , reaches its upper limit (baffle is trying to fill the cavity). In other cases the search stops at sub-optimal points with the same order of standard deviation but with lower average velocity.
2. The location of baffle x_1 , and the spacing between baffles, x_3 , changes accordingly to accommodate for the high limit of x_2 .
3. Pipe radius, x_4 , is close to, but not at, its lower limit since reducing the pipe radius corresponds to a lower average velocity while increasing it can make flow area narrower.
4. Both the radius of the fixed portion of the baffle, x_5 , and length of the extended portion of the baffle x_6 , move toward their upper limit consistently regardless of the initial guess. This is reasonable since observation shows that as the baffle is extended inside the cell, the more the flow follows its walls.

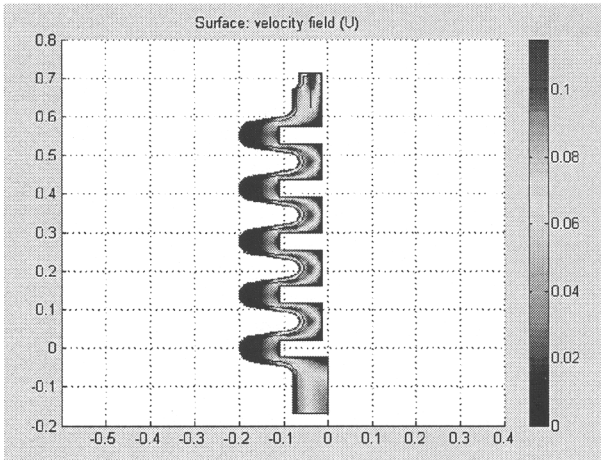


Figure 7. Velocity Field for the Optimized Modified Baffle Design

VII. DESIGN AND FABRICATION OF OPTIMIZED BAFFLE

The CFD plot Figure 7 shows the optimized baffle inside the cavity. The baffle has to be designed in such a way that it could be placed inside the cell. A 3-Dimensional CAD model of the optimized baffle inside the cavity is shown in Fig. 8.

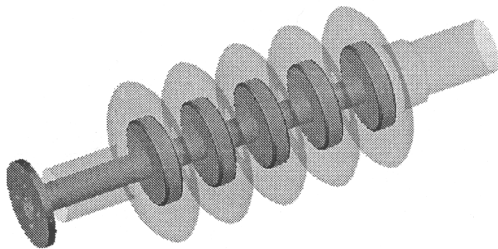


Figure 8. 3-D Model of Optimized baffle inside the cavity

After considering several design alternatives, it is decided to fabricate the baffle as separate sub-assemblies and assemble them inside the cavity, using head and end discs as shown in Figure 9 through Figure 12.

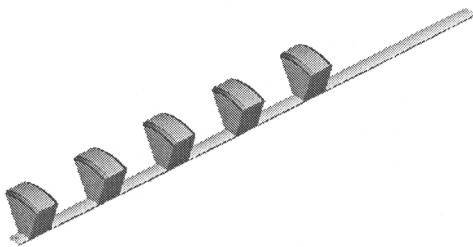


Figure 9. Baffle sub-assembly

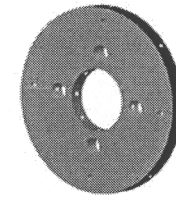


Figure 10. Head



Figure 11. End disc

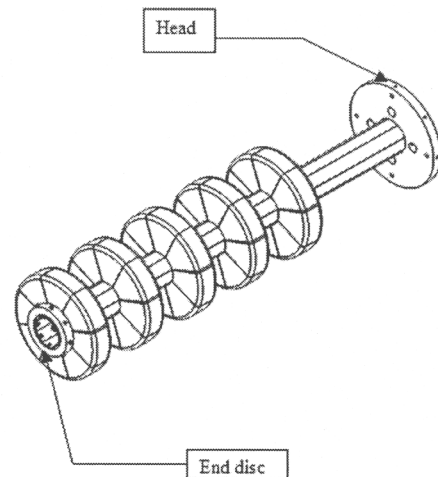


Figure 12. Optimized baffle

VIII EXPERIMENTAL SETUP

Verification of the predicted velocity distributions in the prototype cavity using acid etchant can be hazardous. Fortunately, laminar and turbulent flow distributions can be verified experimentally through dynamic similitude by choosing a substitute fluid that has the same Reynolds number as the desired flow rate to produce similar flow patterns. The velocity of the substitute fluid must be adjusted for differences in fluid density and viscosity. It was decided to use water in the experiment as the substitute fluid. Calculation for velocity of water is based on Equation (11). The data for this equation are listed in Table IV

$$\frac{\rho_e V_e}{\mu_e} = \frac{\rho_w V_w}{\mu_w} \quad (11)$$

Table IV Data for the original setup and the experiment

Density of etching fluid (ρ_e)	1532 kg/m ³
Dynamic viscosity of etching fluid (μ_e)	0.02 kg/m-s
Inlet velocity of etching fluid (V_e)	0.047 m/s
Density of water (ρ_w)	1000 kg/m ³
Dynamic viscosity of water (μ_w)	0.001 kg/m-s

Substituting in Equation (11), the inlet velocity of water is equal to, 0.0036 m/s compared to 0.047m/s (velocity of etching fluid). This corresponds to a flow rate of 43.4 GPH. The CAD layout for the experimental setup is shown in Figure 13. The optimized baffle inside the cavity with dye injection in the first cell is shown in Figure 14.

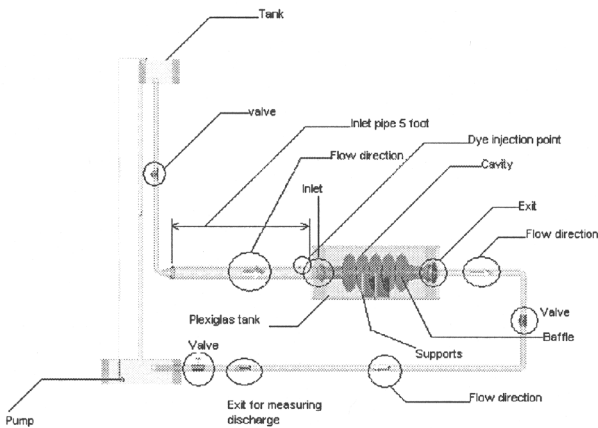


Figure 13. CAD layout of experimental setup

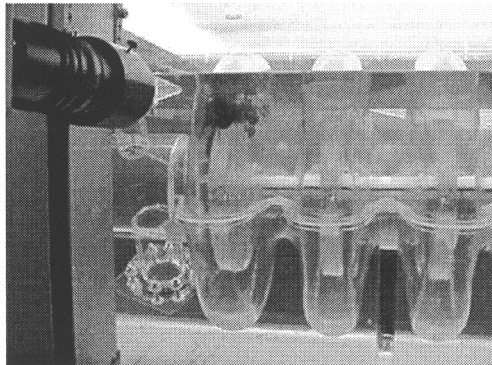


Figure 14. Fabricated optimized baffle inside cavity

IX. EXPERIMENTAL VERIFICATION

This section presents experimental verification of CFD results for both LANL and optimized baffle. This step is done by selecting a streamline at the leading edge of the injected dye near the center of a baffle disc. The location of this streamline is calculated. The velocity of the same streamline at the CFD model is identified then, which should be extremely low. Figure 15 shows the distance between streamline from the leading edge of the dye and the edge of the baffle disc in the first cell. Calibrating the image shows that this distance is 0.0224 m. The

streamline at the same distance in the CFD plot, Figure 16, has a velocity of 0.0022 m/s. similar analysis was done with the optimized baffle. Calibrated image with optimized baffle, Figure 17, shows that the leading edge occurs at a distance of 0.028 m. The streamline velocity value at this location is found from the CFD plot, Figure 18, to be 0.0023 m/s, which is also low. This proves that the optimized baffle helps the flow penetrate into the cell by a distance of 0.028 m from the baffle tip.

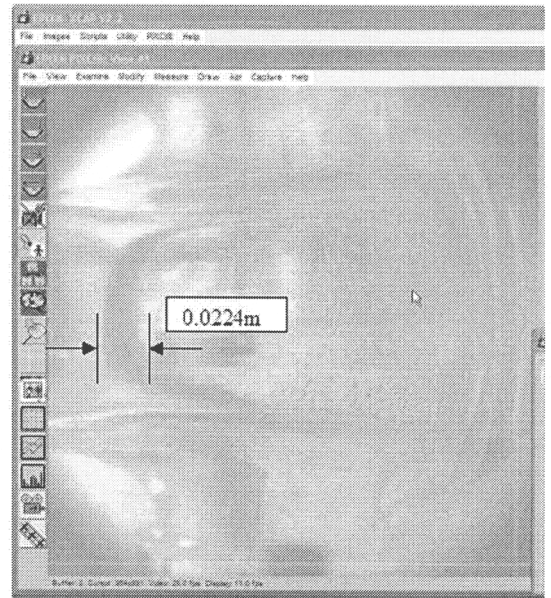


Figure 15 Experimental image of LANL baffle

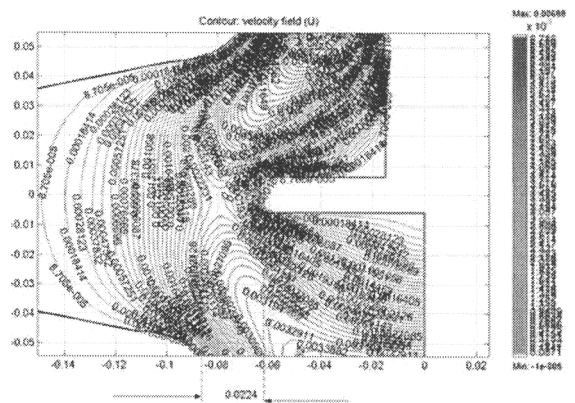


Figure 16 CFD velocity plots for LANL baffle

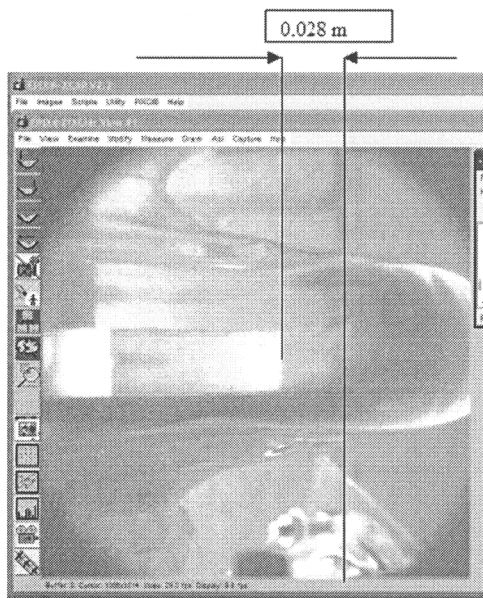


Figure 17 Experimental image of Optimized baffle

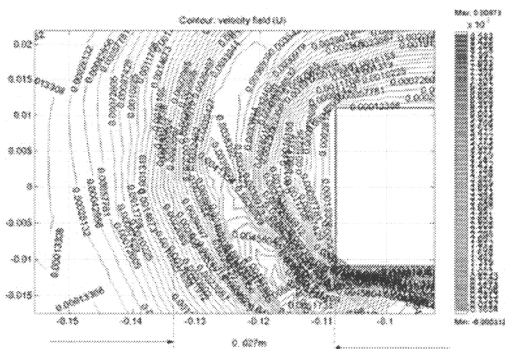


Figure 18 CFD velocity plots for optimized baffle

X. CONCLUSION

This paper presents a method to assess and optimize the quality of chemical etching techniques of niobium cavities when baffle is used to direct the etching fluid along the surfaces of the cavity. A finite element computational fluid dynamics (CFD) model is developed for the etching process. The problem is modeled as a two-dimensional, axi-symmetric, steady state fluid flow problem. The model shows that existing baffle results in etching the iris regions of the cavity than the equator regions, which confirms the observations of Aune et al. [8]. The exit condition is also modified such that the flow leaves the cavity outlet instead of holes in the baffle, which helps in getting rid of backflow and also in maintaining a uniform flow through the entire surface. All ten possible variables of the baffle were identified. A sensitivity analysis was performed. The problem appears to be sensitive to the six variables. The key variables were then optimized to minimize the standard

deviation along the cavity surface while maximizing the average velocity in the same region. The problem is subject to several geometrical constraints to ensure realistic solution to the problem. Some constraints include baffle and internal walls collision detection constraint; mesh quality constraint, and geometrical constraint. Fuzzy Simplex Algorithm improved the initial estimate. The optimized baffle design shows that the average velocity along the walls increases from 0.0482 m/s to 0.0553 m/s and the standard deviation is reduced from 0.2422 m/s to 0.1854 m/s compared to LANL design. To verify the CFD results, an experiment for flow visualization was carried out. The experimental setup uses a transparent prototype of a LANL APT cavity, high-speed CCD camera and a traversing mechanism for positioning the camera. At first, LANL baffle was used. The experimental results confirmed that the optimized baffle design can help the flow penetrate into the cell better than the LANL baffle as predicted by the CFD results.

ACKNOWLEDGMENTS

This work is funded through the University of Nevada, Las Vegas, Advanced Accelerator Applications University Participation Program administered by the Harry Reid Center for Environmental Studies (U.S. Department of Energy Grant No. DE-FG04-2001AL67358). The authors would also like to acknowledge the continuous help and interaction of LANL personnel, especially Dr. K. C. Dominic Chan.

REFERENCES

1. "A Roadmap for Developing Accelerator Transmuting of Waste (ATW) Technology," DOE/RW-0519, October 1999.
2. E. Chiaveri, "Large-Scale Industrial Production of Superconducting Cavities," EPAC96, pp. 200-204.
3. V. Palmieri, "Review of Fabrication of SC Cavity Structures," Proceedings of LINAC98, p. 697-700.
4. P. Kneisel, "Surface Preparation for Niobium," First Workshop on RF Superconductivity, Karlsruhe, Germany, 1980, p. 27-40.
5. M. Ono, "Development of TESLA-type Cavity at KEK," Proceedings of IEEE Particle Accelerator Conference, 1995, p. 1629-1631.
6. P. Kneisel and V. Palmieri, "Development of seamless niobium cavities for accelerator applications," Proceedings of IEEE Particle Accelerator Conference, 1999, p. 943-945.
7. W. Singer et al., "Hydro Forming of TESLA Cavities at DESY," Proceedings of EPAC 2000, p. 324-326.
8. B. Aune et al., "The Superconducting TESLA Cavities," Phys. Rev. Spec. Top. Accel. Beams 3 (2000) 092001.
9. Trabia, M. and X. Lu, "A Fuzzy Adaptive Simplex Search Optimization Algorithm," ASME Journal of Mechanical Design, 123, June 2001, p. 216-225.